Indian Journal of Chemistry
Vol. 61, June 2022, pp. 617-622

Computational investigation of the solvent and temperature effects on the tautomerization of 7-amino-1,3-dioxo-2,5-diphenyl-2,3-dihydro-1*H*, 5*H*-pyrazolo[1,2-a][1,2,4]triazole-6-carbonitrile

Zohreh Khanjari[a], Bita Mohtat*[a], Reza Ghiasi[b], Hoorieh Djahaniani[b] & Farahnaz Kargar Behbahani[a]

[a] Department of Chemistry, Karaj Branch, Islamic Azad University, Karaj, Iran

[b] Department of Chemistry, East Tehran Branch, Islamic Azad University, Tehran, Iran

E-mail: b_mohtat@yahoo.com

Received 21 September 2020; accepted (revised) 23 December 2021

This research examines the effects of solvent polarity and temperature on the tautomerization of 7-amino-1,3-dioxo-2, 5-diphenyl-2,3-dihydro-1*H*,5*H*-pyrazolo[1,2-a][1,2,4]triazole-6-carbonitrile at CAM-B3LYP/6-311G (d,p) level of theory. The selected solvents are *n*-hexane, diethyl ether, pyridine, ethanol, methanol, and water. The solvent effects have been examined by the self-consistent reaction field theory (SCRF) based on conductor-like polarizable continuum model (CPCM). The solvent effects have been explored on the energy barrier, frontier orbitals energies, and HOMO-LUMO gap. Dependencies of thermodynamic parameters (ΔG andΔH) on the dielectric constants of solvents have also been tested. Specifically, the temperature dependencies of the thermodynamics parameters have been studied within 100-1000 K range. The rate constant of the tautomerism reaction is computed from 300 to 1200 K, in the gas phase.

Keywords: Tautomerism, solvent effect, temperature effect, thermodynamics parameters, rate constant

Compounds containing pyrazoles[1] are known to display diverse pharmacological activities such as antibacterial, antifungal, anti-inflammatory, analgesic, and antipyretic[2]. A number of heterocyclic compounds fused with pyrazole are known for their varied biological and industrial applications[3]. The pyrazolotriazole are precursors for photosensitive materials (e.g. inks and toners)[4] and ingredients in cosmetics[5]. Preparation of 7-amino-1,3-dioxo-1,2,3,5-tetrahydropyrazolo [1,2-a][1,2,4]triazole has been reportedusing magnetic Fe_3O_4 nanoparticles coated with (3 aminopropyl)-triethoxysilane as catalyst[1] for the formation of the 7 amino-1,3-dioxo-1,2,3,5-tetrahydropyrazolo[1,2-a][1,2,4]triazoles[6].

Many investigations have been reported about tautomerization reactions[7-17]. Also, solvent polarity importance on the structure and properties of the molecules have been studied using quantum mechanics tools[18-28].

In this study, we investigate Solvent and Temperature effects on the tautomerization of 7 amino-1,3-dioxo-2,5-diphenyl-2,3-dihydro-1*H*,5*H*-pyrazolo[1,2-a][1,2,4]triazole-6-carbonitrile at the CAM-B3LYP/6-311G(d,p) level of theory.

Computational Methods

Optimization and vibrational analysis were done using Gaussian 09 software package[29]. The standard 6-311G (d, p) basis set[30-33] was considered for the elements. CAM-B3LYP functional was used for optimizing the geometries of the compound. This functional is Handy et al.'s long range corrected version of B3LYP using the Coulomb-attenuating method[34]. The identities of the optimized structures as an energy minimum were confirmed via vibrational analysis.

For the solvation impact study, we utilized a self-consistent reaction field (SCRF) approach, using conductor-like polarizable continuum model (CPCM)[35,36].

The identity of the reactants, transition states, and products was confirmed through vibrational analysis. All the transition states (TS) were checked by the intrinsic reaction coordinate (IRC) analysis at the same level of theory[37-40].

Calculations of the population analysis were bone via the natural bond orbital (NBO) method[41] using the NBO 3.1 program[42] implemented in the Gaussian 09 package.

Gpop program was used for computing the reaction rate parameters[43]. The temperature dependence of the

rate constants was investigated within 300−1200 K using transition state theory (TST) based on statistical thermodynamics. Further, the tunneling effect was considered by assuming asymmetric Eckart potential[44] and Shavitt's correction[45] the corresponding correction factor for corrections of the rate constants values.

The Eckart potential function is often used to estimate quantum mechanical tunneling corrections to theoretically determined chemical rate constants. Eckart's potential has the following form:

$$V = -\frac{y\left[\frac{A-B}{1-y}\right]}{1-y}; \quad \ldots (1)$$

$$y = -\exp\left(\frac{2\pi x}{L}\right); A = V_1 - V_2; B = \left(V_1^{\frac{1}{2}} + V_2^{\frac{1}{2}}\right)^2; L = 2\pi\left(\frac{2}{F^*}\right)^{\frac{1}{2}}\left(V_1^{-\frac{1}{2}} + V_2^{-\frac{1}{2}}\right)^{-1}$$

The potential has the limiting value of zero when x→-∞, goes through a single maximum of height V_1 as x increases, and has a limiting value of V_1 - V_2 as x→+∞. F* is the second derivative of V at its maximum.

Shavitt recommended a simple equation for the tunneling correction:

$$Q_{tunnel} = 1 - \frac{1}{24}\left[\frac{h\nu^*}{k_B T}\right]^2\left[1 + \frac{k_B T}{E_0}\right]; \quad \ldots (2)$$

Where,ν*, k_B, h, and E_0represent the imaginary frequency of the activated complex at the top of the barrier, Boltzmann's constant, Plank's constant, and the barrier height corrected for zero-point energy for the reaction, respectively.

Results and discussion

Energy aspects

Figure 1 presents the structures of 7-amino-1,3-dioxo-2,5-diphenyl-2,3-dihydro-1*H*,5*H*-pyrazolo[1,2-a][1,2,4]triazole-6-carbonitrile**(I)**,5-imino-1,3-dioxo-2,7-diphenyltetrahydro-1*H*,5*H*-pyrazolo[1,2-a][1,2,4]triazole-6-carbonitrile **(II)**and transition state **(TS)**of this tautomers. Table I reports the total energy and solvation energy values of these molecules in the gas and solution phases forn-hexane, diethyl ether, pyridine, ethanol, methanol, and water. These values show that **II**-isomer is more stable than **I**-isomer in both gas and solution phases. As can be seen, the stability of the molecules increases in the solution phase, and its stability grows in more polar solvents. Thus, in the presence of solvent, the reacting molecule is stabilized energetically through electrostatic interaction with the solvent. The solvation energy values were computed based on the

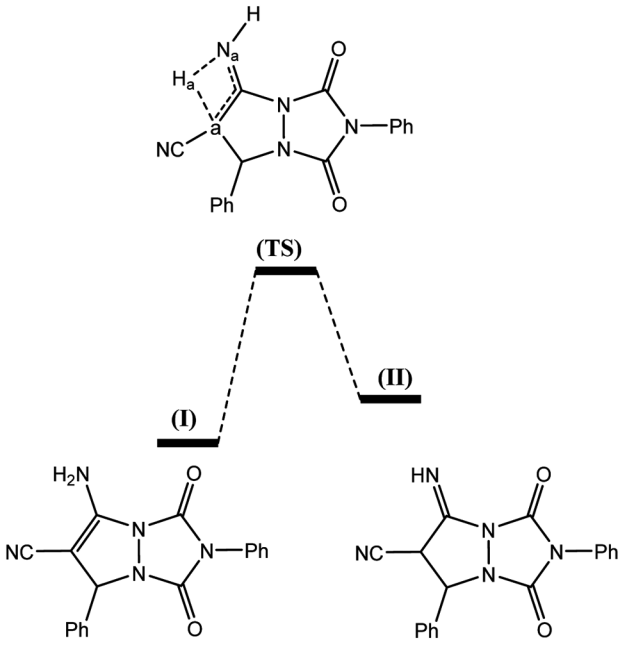

Figure 1 — the structures of 7-amino-1,3-dioxo-2,5-diphenyl-2,3-dihydro-1*H*,5*H*-pyrazolo[1,2-a][1,2,4]triazole-6-carbonitrile **(I)**, 5-imino-1,3-dioxo-2,7-diphenyltetrahydro-1*H*,5*H*-pyrazolo[1,2-a][1,2,4]triazole-6-carbonitrile **(II)** and transition state **(TS)** of this tautomers

Table I — total energy (E, a.u) and dipol moment values (μ, Debye) of tautomers of 7-amino-1,3-dioxo-2,5-diphenyl-2,3-dihydro-1*H*,5*H*-pyrazolo[1,2-a][1,2,4]triazole-6-carbonitrile and transition state between them (a.u) in the gas and solution phases.**ΔE**‡ and **ΔE$_r$** are energy barrier and reaction energy of the tautomerisation (kcal/mol). ω_{lowest} is imaginary wave-number of transition state (in cm^{-1}). ε is dielectric constant of solvents.

Phase	ε	E(I)	E(TS)	E(II)	μ(I)	μ(II)	ΔE‡	ΔE$_r$	ω_{lowest}
Gas	–	−1117.6485	−1117.4482	−1117.6695	4.24	3.41	125.68	−13.19	−1289.4
n-Hexane	1.89	−1117.6600	−1117.4593	−1117.6783	4.77	3.97	125.90	−11.52	−1260.2
Diethyl ether	4.34	−1117.6685	−1117.4676	−1117.6848	5.20	4.45	126.01	−10.24	−1239.9
Pyridine	12.30	−1117.6735	−1117.4726	−1117.6886	5.48	4.78	126.05	−9.45	−1226.5
Ethanol	24.30	−1117.6747	−1117.4739	−1117.6895	5.55	4.87	126.05	−9.26	−1222.5
Methanol	32.63	−1117.6751	−1117.4742	−1117.6897	5.57	4.89	126.05	−9.21	−1221.4
Water	78.54	−1117.6757	−1117.4748	−1117.6902	5.61	4.94	126.05	−9.11	−1219.4

difference between energetic values in the gas phase and solution phase. These values are provided in Table I. As can be seen, these values diminished by increasing the dielectric constant of solvents.

The transition state geometry suggested for the studied tautomerization reaction is depicted in Figure 1. TS has a four-membered ring structure. According to the frequency analysis calculations, all TSs have distinctive imaginary frequency. These values are outlined in Table I.

The changes in the total energy upon alteration of the C_a-H_a and N_a-H_a bond distances along the IRC path are shown in Figure 2 in the gas phase. It can be observed that the N_a-$H_a$bond rapidly lengthens from the reactant side. On the other hand, the C_a-H_a bond rapidly shortens from the reactant side. There are identical variations in the presence of other solvents.

The activation energy ($\mathbf{\Delta E^{\ddagger}}$) and reaction energy change ($\mathbf{\Delta E_r}$) values of the tautomerization are listed in Table I, where larger $\mathbf{\Delta E^{\ddagger}}$ and $\mathbf{\Delta E_r}$ values are found in the solution phase than in the gas phase. These values increase in more polar solvents.

Thermodynamics

Solvent effects

The thermodynamic parameters of the studied tautomerization reaction are outlined in Table II. The negative values of the reaction free energy ($\mathbf{\Delta G_r}$) reveal that the studied reaction is spontaneous. It can be seen that this reaction is more appropriate in the solution phase as compared to the gas phase. This reaction is more appropriate in more polar solvents.

In addition, as the results show, the activation free energy values ($\Delta G^{\ddagger}$) are larger in the solution phase than in the gas phase. The more polar solvents have led to greater $\Delta G^{\ddagger}$ values.

The enthalpy values of the reaction ($\mathbf{\Delta H_r}$) are listed in Table II. The negative values of the studied reaction show that this reaction is exothermic.
The results also indicate that the activation enthalpy values ($\Delta H^{\ddagger}$) are larger in the solution phase than in the gas phase. The more polar solvents have led to greater $\Delta H^{\ddagger}$ values.

A plot of the barrier heights ($\mathbf{\Delta E^{\ddagger}}$) versus $\mathbf{\Delta H_r}$ reveals that $\mathbf{\Delta E^{\ddagger}}$ varies linearly with $\mathbf{\Delta H_r}$ for all the processes considered. There is a linear correlation between $\mathbf{\Delta E^{\ddagger}}$ and $\mathbf{\Delta H_r}$ (Figure 3):

$\Delta H_r = 14.8\ \Delta E^{\ddagger} - 1874.9;$ $R^2 = 0.9632$

Temperature effects

The thermodynamics parameters of the studied tautomerization reaction are listed in Table III within the 100-1000 K temperature range. The negative values of the reaction free energy (ΔG_r) show that the studied reaction is spontaneous within the studied temperature range. It can be seen that this reaction is more appropriate at higher temperatures. There is a good linear correlation between ΔG_r values with temperature (T):

$\Delta G_r = -0.0015\ T - 12.786;$ $R^2 = 0.9809$

Table II — Thermodynamic parameters of tautomerism of 7-amino-1,3-dioxo-2,5-diphenyl-2,3-dihydro-1*H*,5*H*-pyrazolo [1,2-a][1,2,4]triazole-6-carbonitrile in gas phase and various solvents.

Phase	$\Delta G^{\ddagger}$	ΔG_r	$\Delta H^{\ddagger}$	ΔH_r
Gas	122.19	−13.20	121.46	−12.87
n-Hexane	122.35	−11.62	121.72	−11.33
Diethyl ether	122.25	−10.50	121.82	−10.18
Pyridine	122.37	−9.85	121.85	−9.46
Ethanol	122.43	−9.68	121.86	−9.28
Methanol	122.45	−9.65	121.86	−9.23
Water	122.49	−9.61	121.86	−9.15

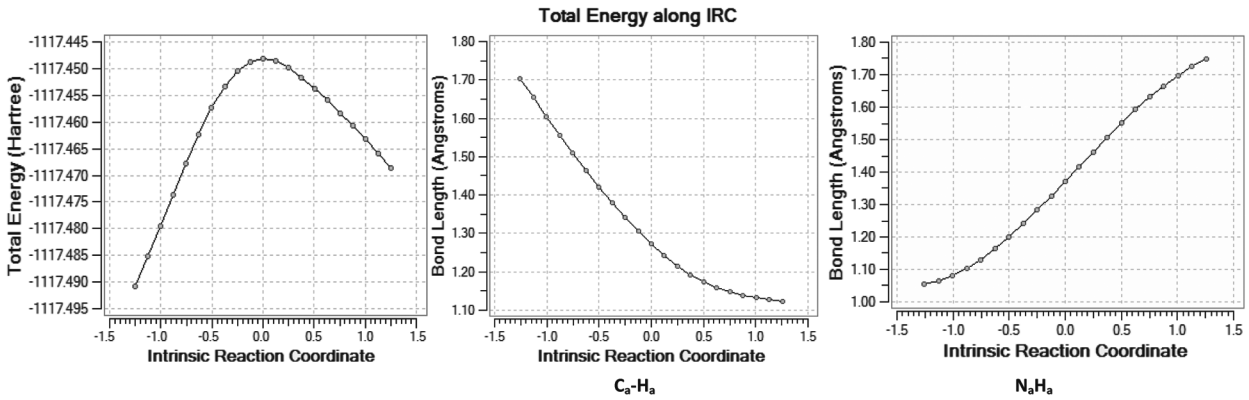

Figure 2 — Energy and bond distances versus reaction coordinate (amu$^{1/2}$. Bohr) in thetautomerization reaction

In addition, as the results show, the activation free energy values ($\Delta G^{\ddagger}$) are larger at higher temperatures. There is a good linear correlation between $\Delta G^{\ddagger}$values with temperature (T):

$\Delta G^{\ddagger} = 0.0025\ T + 121.45;$ $R^2 = 0.9982$

The enthalpy values of the reaction ($\mathbf{\Delta H_r}$) are provided in Table III within the 100-1000 K temperature range. The negative values of the studied reaction show that this reaction is exothermic within the studied temperature range.$\mathbf{\Delta H_r}$ values increase with temperature rise. There is not a good linear correlation between $\mathbf{\Delta H_r}$ values and temperature (T):

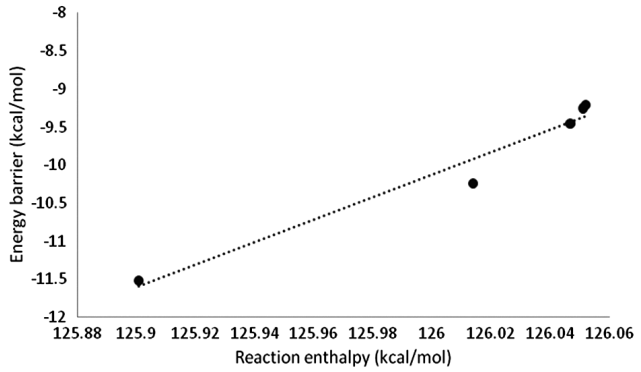

Figure 3 — Linear correlation between barrier heights ($\mathbf{\Delta E^{\ddagger}}$) versus $\mathbf{\Delta H_r}$ of the tautomerization reaction.

Table III — Thermodynamic parameters of tautomerism of 7-amino-1,3-dioxo-2,5-diphenyl-2,3-dihydro-1*H*,5*H*-pyrazolo [1,2-a][1,2,4]triazole-6-carbonitrile in various temperatures.

T (K)	$\Delta G^{\ddagger}$	ΔG_r	$\Delta H^{\ddagger}$	ΔH_r
100	121.78	−13.07	121.63	−13.03
200	121.96	−13.12	121.53	−12.99
300	122.19	−13.20	121.46	−12.87
400	122.44	−13.33	121.43	−12.75
500	122.70	−13.49	121.40	−12.66
600	122.96	−13.66	121.39	−12.60
700	123.22	−13.84	121.36	−12.56
800	123.49	−14.03	121.33	−12.54
900	123.76	−14.22	121.29	−12.53
1000	124.03	−14.40	121.24	−12.53

$\Delta H_r = 0.0006\ T - 13.038;$ $R^2 = 0.8967$

On the other hand, these parameters are fitted with a quadratic equation:

$\Delta H_r = -8\times 10^{-7}\ T^2 + 0.0014\ T - 13.203;$ $R^2 = 0.9848$

In addition, as the results show, the activation enthalpy values ($\Delta H^{\ddagger}$) are larger at lower temperatures. There is a good linear correlation between $\mathbf{\Delta H^{\ddagger}}$ values and temperature (T):

$\mathbf{\Delta H^{\ddagger}} = -0.0004\ T + 121.61;$ $R^2 = 0.9364$

On the other hand, these parameters are fitted with a quadratic equation:

$\mathbf{\Delta H^{\ddagger}} = 2 \times 10^{-7}\ T^2 - 0.0006\ T + 121.65;$ $R^2 = 0.9586$

Dipole moment

As a larger dipole moment can increase the overall energy corresponding to a conformation, the population corresponding to the conformation with a larger dipole moment can be reduced compared with the conformation with a less dipole moment[46]. A greater dipole moment is associated with greater charge distribution (polarization). Thus, the conformations with greater dipole moments can be softer than those with smaller dipole moments.

The results show that the dipole moments of the **II**-isomer compounds are smaller compared with their **I**-isomer (Table I).

On the other hand, these values show that dipole moment values of I and II-isomers increase in the solution phase as compared to the gas phase. These values increase in the presence of more polar solvents. The elevation of the dipole moment values is attributed to long range interactions solvent with the solute molecules.

Molecular orbital analysis

The energies of the frontier orbitals (HOMO, LUMO) and the corresponding HOMO–LUMO energy gaps values of the investigated molecules are given in Table IV.

Table IV — Frontier orbital energy and HOMO-LUMO gap values (eV) of tautomers of 7-amino-1,3-dioxo-2,5-diphenyl-2,3-dihydro-1*H*,5*H*-pyrazolo[1,2-a][1,2,4]triazole-6-carbonitrile.

	I-isomer			II-isomer		
Phase	E(HOMO)	E(LUMO)	Gap	E(HOMO)	E(LUMO)	Gap
Gas	−8.34444	0.00381	8.34825	−7.7768	0.161093	7.937896
n-Hexane	−8.43124	0.019864	8.451104	−7.74007	0.176331	7.916399
Diethyl ether	−8.47478	0.027484	8.502264	−7.71122	0.188032	7.899255
Pyridine	−8.46961	0.033198	8.502808	−7.6919	0.195379	7.887282
Ethanol	−8.46798	0.035103	8.503083	−7.68673	0.197284	7.884017
Methanol	−8.46771	0.035647	8.503357	−7.68537	0.1981	7.883473
Water	−8.46689	0.037008	8.503898	−7.68265	0.199189	7.88184

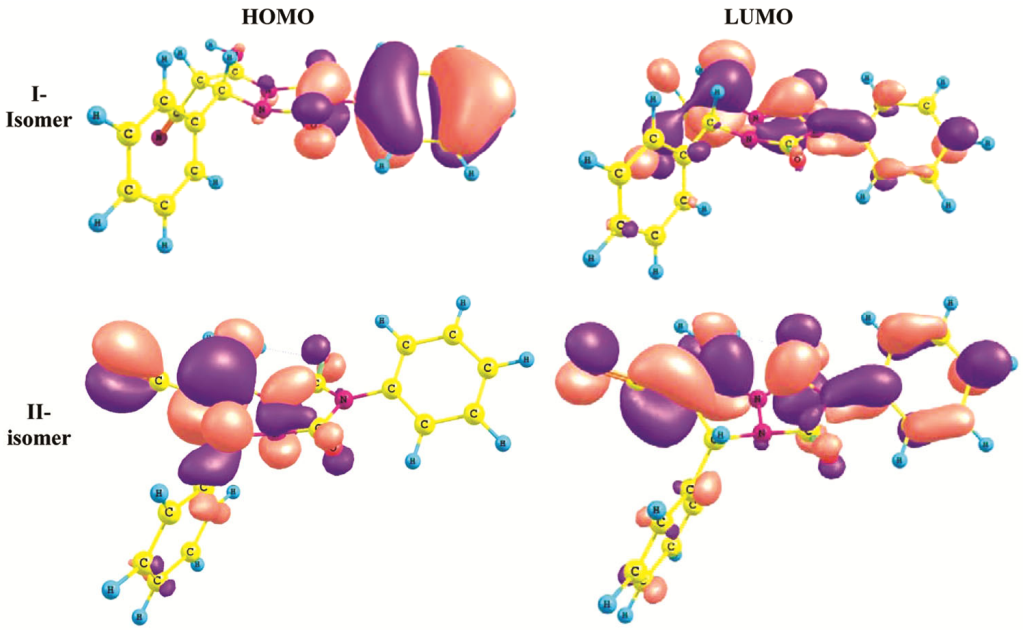

Figure 4 — Plots of frontier orbitals of **I** and **II**- isomers

As seen in Table IV, HOMO of **I**-isomer is has been stabilized in the solution phase as compared to the gas phase. On the other hand, LUMO of **I**-isomer, HOMO, and LUMO of **II**-isomer has been destabilized in the solution phase as compared to the gas phase. The plots of frontier orbitals of **I** and **II**- isomers are shown in Figure 4.

As shown in Table IV, HOMO-LUMO gaps values of I-isomer are larger in the solution phase as compared to the gas phase. In contrast, HOMO-LUMO gaps values of II-isomer are smaller in the solution phase as compared to the gas phase.

Calculation of the rate constants

No direct experimental investigation has reported the rate constant of the investigated tautomerization reaction at any temperature, to the best of our knowledge.The rate constant values of the studied isomerization reaction are summarized in Table V. Furthermore, the tunneling factor is considered for calculations of the rate constant values. Asymmetric Eckart potential and Shavitt's correction the corresponding correction factor of tunneling are assumed for corrections of the rate constants (Table V). These values have been calculated in the gas phase and within the temperature range of 300-1200 K. Th equations fitted to the gas phase Arrhenius equation are collected in Table VI.

Table V — The gas phase calculated rate constants for studied reactions (s^{-1}): (a) excluding tunneling factor, and corrected rate constants for tunneling by assuming (b) asymmetric Eckart potential, (c) Shavitt's correction.

T	a	b	c
300	5.59×10^{-77}	1.11×10^{-75}	1.45×10^{-76}
400	9.95×10^{-55}	3.09×10^{-45}	1.89×10^{-54}
500	2.33×10^{-41}	4.49×10^{-41}	3.68×10^{-41}
600	1.96×10^{-32}	3.04×10^{-32}	2.75×10^{-32}
700	$4.77E\times10^{-26}$	6.52×10^{-26}	6.18×10^{-26}
800	2.98×10^{-21}	3.77×10^{-21}	3.65×10^{-21}
900	1.62×10^{-17}	1.95×10^{-17}	1.91×10^{-17}
1000	1.58×10^{-14}	1.84×10^{-14}	1.82×10^{-14}
1100	4.47×10^{-12}	5.06×10^{-12}	5.01×10^{-12}
1200	4.95×10^{-10}	5.49×10^{-10}	5.45×10^{-10}

Table VI — Fitted equations to the gas phase Arrhenius equation for studied reactions: (a) excluding tunneling factor, and corrected rate constants for tunneling by assuming (b) asymmetric Eckart potential, (c) Shavitt's correction.

$$k_{gas} = A \exp\left(-\frac{E\ kJ.mol^{-1}}{T}\right)$$

	(a)		(b)		(c)	
X	A	E/R	A	E/R	A	E/R
Cp	9.24×10^{12}	61664.19	3.32×10^{12}	60630.7	7.45×10^{12}	61319.28

Conclusion

Computational investigation of the effects of solvent polarity and temperature on the tautomerization of 7-amino-1,3-dioxo-2,5-diphenyl-2,3-dihydro-1*H*,5*H*-pyrazolo[1,2 a][1,2,4]triazole-6-carbonitrile were studied at CAM-B3LYP/6-311G (d,p) level of theory reveal that:

(i) I-isomer was more stable than I-isomer in both gas and solution phases.

(ii) $\Delta E^{\ddagger}$ and ΔE_r values were larger in the solution phase than in the gas phase. These values increased in more polar solvents.

(iii) The negative values of ΔG_r and ΔH_r showed that the studied reaction was exothermic, respectively in both gas and solution phase.

(iv) Dipole moment values of I and II-isomers increased in the solution phase when compared to the gas phase. These values increased in the presence of more polar solvents.

(v) HOMO-LUMO gaps values of I-isomer were larger in the solution phase than in the gas phase. In contrast, HOMO-LUMO gaps values of II-isomer were smaller in the solution phase as compared to the gas phase.

References

1 Haddad N, Salvango A & Busacca C, *Tetrahedron Lett*, 45 (2004) 5935.

2 Tanitame A, Oyamada Y, Ofugi K, Fujimoto M, Iwai N, Hiyama Y, Suzuki K, Ito H,Terauchi H, Kawasaki M, Nagai K, Wachi M & Yamagishi M J I, *J Med Chem*, 47 (2004) 3693.

3 Varano F, Catarzi D, Colotta V, Lenzi O, Filacchioni G, Galli A & Costagli C, *Bioorg Med Chem*, 16 (2008) 2617.

4 Bailey J, *J Chem Soc Perkin Trans 1*, (1977) 2047.

5 Plos G & Lagrange A, *Eur Pat Appl Patent EP*, 1062937 (2000).

6 Shaterian H R & Moradi F, *Res Chem Intermed*, 41 (2015) 223.

7 Ghiasi R, Fashami M Z & Hakimioun A H, *J Theor Comput Chem*, 13 (2014) Article 1450023.

8 Meshhal M M, Shibl M F, El-Demerdash S H & El-Nahas A M, *Comput Theor Chem*, 1145 (2018) 6.

9 Tejchman W & Zborowski K, *Comput Theor Chem*, 1087 (2016) 6

10 Özdemir N, *Comput Theor Chem*, 1086 (2016) 12

11 Umadevi V, Priya A M & Senthilkumar L, *Comput Theor Chem*, 1068 (2015) 149.

12 Lukmanov T, Ivanov S P, Khamitov E M & Khursan S L, *Comput Theor Chem*, 1023 (2013) 38.

13 Karpińska G & Dobrowolski J C, *Comput Theor Chem*, 1052 (2015) 58.

14 Karpińska G, Mazurek A P & Dobrowolski J C, *Comput Theor Chem*, 972 (2011) 48.

15 Mohammadpour M, Zborowski K K, Heidarpoor S, Żuchowski G & Proniewicz L M, *Comput Theor Chem*, 1078 (2016) 96.

16 Hoang V H, Le C T, Nguyen N T & Le V H, *Comput Theor Chem*, 1043 (2014) 31.

17 Karpińska G & Dobrowolski J C, *Comput Theor Chem*, 1005 (2013) 35.

18 Saraf S H & Ghiasi R, *Russ J Phys Chem A*, 94 (2020) 1047.

19 Milani N N, Ghiasi R & Forghaniha A, *J Appl Spectrosc*, 86 (2020) 1123.

20 Kiani M, Ghiasi R, Pasdar H & Mirza B, *Russ J Phys Chem A*, 94 (2020) 345.

21 Ghiasi R, Rahimi M & Jamaat P R, *Russ J Inorg Chem*, 65 (2020) 69.

22 Ansari E S, Ghiasi R & Forghaniha A, *Chemical Methodologies*, 4 (2020) 220.

23 Nilchi M, Ghiasi R & Nasab E M, *J Chil Chem Soc*, 64 (2019) 4360.

24 Mahmoudzadeh G, Ghiasi R & Pasdar H, *Russ J Phys Chem A*, 93 (2019) 2244.

25 Rezazadeh M, Ghiasi R & Jamehbozorgi S, *J Struct Chem*, 59 (2017) 245.

26 Rezazadeh M, Ghiasi R & Jamehbozorgi S, *J Appl Spectrosc*, 85 (2018) 526.

27 Rahimi M & Ghiasi R, *J Mol Liq*, 265 (2018) 164.

28 Ghiasi R, *J Mol Liq*, 264 (2018) 616.

29 Frisch M J, Trucks G W, Schlegel H B, Scuseria G E, Robb M A,Cheeseman J R, Scalman G, Barone V, Mennucci B, Petersson G A, Nakatsuji H, Caricato M, Li X, Hratchian H P, Izmaylov A F, Bloino J, Zheng G, Sonnenberg J L, Hada M, Ehara M, Toyota K, Fukuda R, Hasegawa J, Ishida M, T Nakajima, Honda Y, Kitao O, Nakai H, Vreven T, Montgomery J A, Jr , Peralta J E, Ogliaro F, Bearpark M, Heyd J J, Brothers E, Kudin K N, Staroverov V N, Kobayashi R, J Normand, Raghavachari K, Rendell A, Burant J C, Iyengar S S, J Tomasi, Cossi M, Rega N, Millam J M, Klene M, Knox J E, Cross J B, Bakken V, Adamo C, Jaramillo J, Gomperts R, Stratmann R E, Yazyev O, Austin A J, Cammi R, Pomelli C, Ochterski J W, Martin R L, Morokuma K, Zakrzewski V G, Voth G A, Salvador P, Dannenberg J J, Dapprich S, Daniels A D, Farkas O, Foresman J B, Ortiz J V, Cioslowski J, Fox D J, *Gaussian 09*, Revision A 02; Gaussian, Inc Wallingford CT, 2009.

30 Hay P J, *J Chem Phys*, 66 (1977) 4377.

31 Krishnan R, Binkley J S, Seeger R & Pople J A, *J Chem Phys*, 72 (1980) 650.

32 McLean A D & Chandler G S, *J Chem Phys*, 72 (1980) 5639.

33 Wachters A J H, *J Chem Phys*, 52 (1970) 1033.

34 Yanai T, Tew D P & Handy N C, *Chem Phys Lett*, 393 (2004) 51.

35 Barone V & Cossi M, *J Phys Chem* A, 102 (1998) 1995.

36 Cossi M, Rega N, Scalmani G & Barone V, *J Comput Chem*, 24 (2003) 669.

37 Fukui K, *Acc Chem Res*, 14 (1981) 363.

38 Fukui K, *J Phys Chem*, 74 (1970) 4161.

39 Gonzalez C & Schlegel H B, *J Phys Chem*, 94 (1990) 5523.

40 Gonzalez C & Schlegel H B, *J Chem Phys*, 90 (1989) 2154.

41 Reed A E, Curtiss L A & Weinhold F, *Chem Rev*, 88 (1988) 899.

42 Glendening E D, Reed A E, Carpenter J E & Weinhold F, *NBO Version 3 1*, Madison 1988

43 Miyoshi A, *Gaussian Post Processor (GPOP)*, University of Tokyo Tokyo, 2010.

44 Garrett B C & Truhlar D G, *J Phys Chem*, 83 (1979) 2921.

45 Shavitt I, *J Chem Phys*, 31 (1959) 1359.

46 Perrin C L, Armstrong K B & Fabian M A, *J Am Chem Soc*, 116 (1994) 715.